Electronic Supplementary Material (ESI) for *Journal of Materials Chemistry A*

Nanoionic Transport and Electric Double Layer Formation at the Electrode/Polymer Interface for High Performance Supercapacitors

Karthik Krishnan,* Premkumar Jayaraman, Subramanian Balasubramanian, and

Ulaganathan Mani

Council of Scientific and Industrial Research (CSIR), Central Electrochemical Research Institute (CECRI), Karaikudi 630 003, India

Address correspondence to: karthikk@cecri.res.in

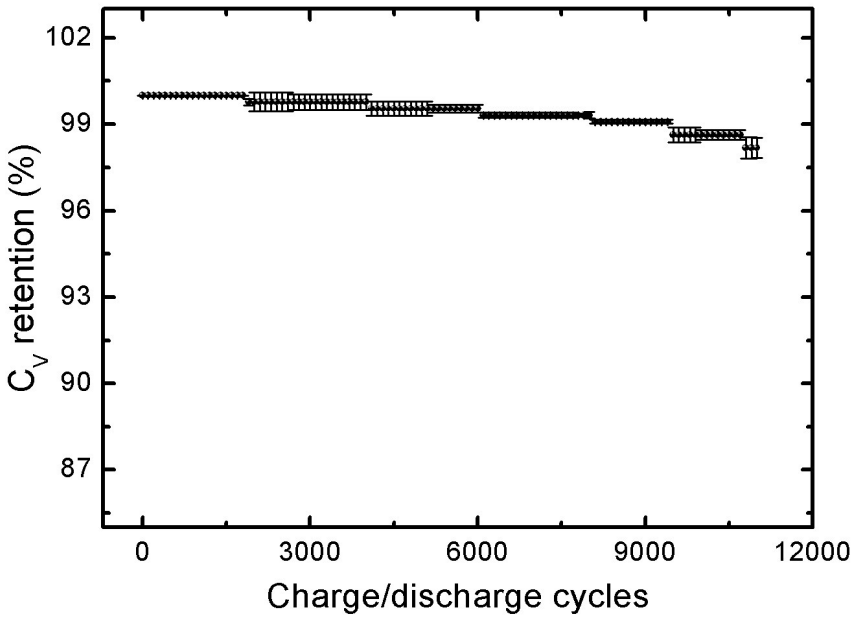

Fig. S1 Capacitance retention of a single-cell planar MSC device with 11000 continuous charge–discharge cycles (error bar value is estimated using three different planar MSC with similar device configuration).

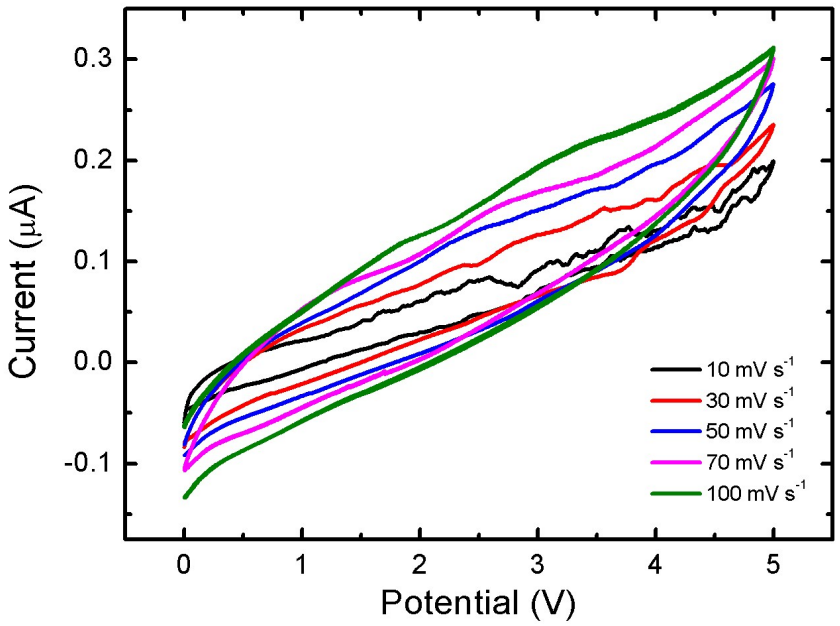

Fig. S2 Scan rate dependent CV plots of the planar MSC device comprises of five series cells at higher cell voltage (5 V).

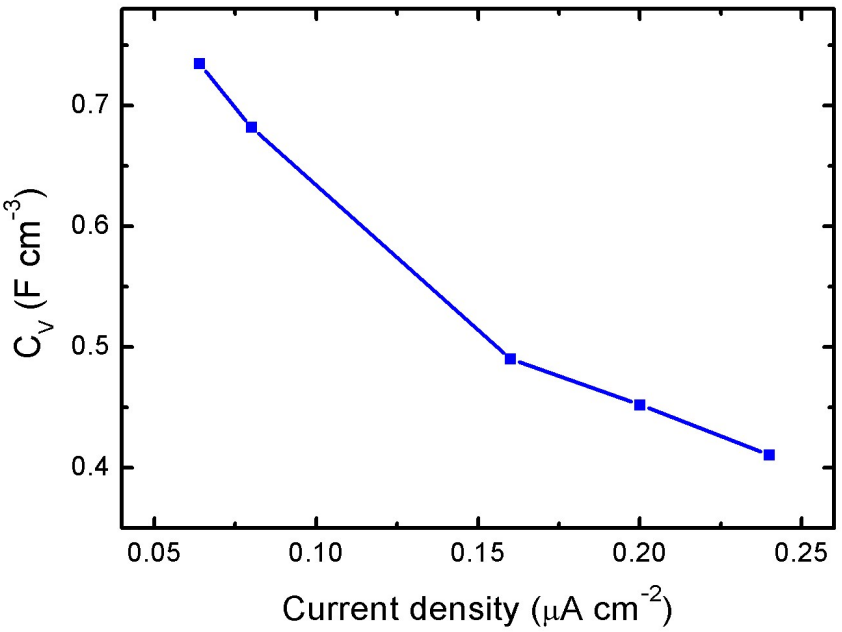

Fig. S3 Current density dependent volumetric capacitance (C_V) of the planar MSC device (contribution of each cell out of five series cells), estimated using GCD plots.

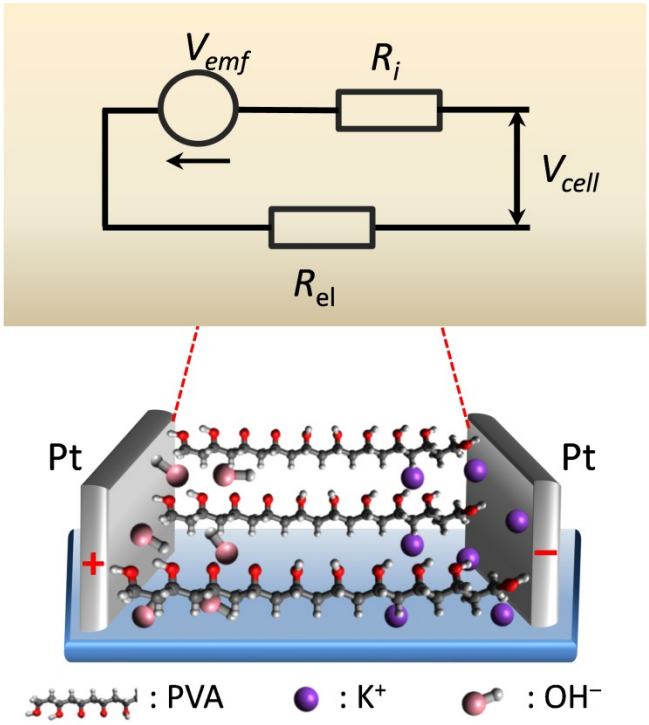

Fig. S4 Schematics of the Pt/PVA–KOH/Pt device and its equivalent circuit model. The cell volatge is estimated using the V_{emf} and the contribution of partial electronic component. R_i and R_{el} are the ionic and electronic resistances, respectively.

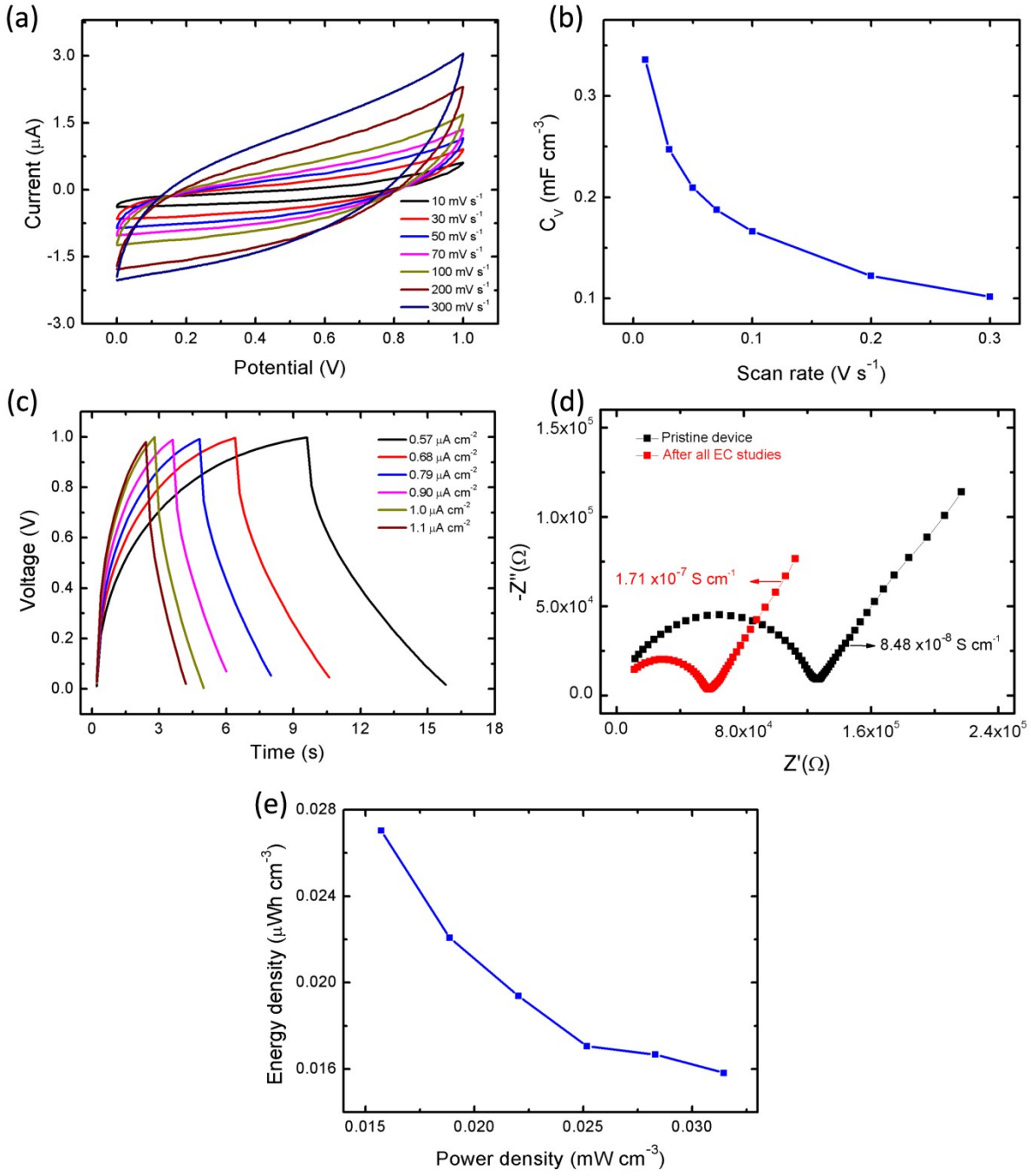

Fig. S5 (a) CV curves of a bulk SC device as function of scan rates (b) Scan rate dependent volumetric capacitance (C_V) that obtained using CV data, (c) Charge–discharge profiles of the device with various current densities (d) Nyquest plots of the bulk SC device (thickness of PVA-KOH ≈ 0.18 mm), measured before (pristine state) and after all electrochemical (EC) studies, and (e) the plot between power and energy density of bulk SC device.

1. Electrochemical performance of bulk Pt/PVA-KOH/Pt SC. The electrochemical performance of the stacked bulk Pt/PVA-KOH/Pt SC using bulk electrolyte (0.18 mm) was studied by two electrode configuration. The CV measurement was performed with a potential window of 0–1 V and scan rate varied from 10 to 300 mV s^{-1}. Fig. S5a represent the CV plots of bulk SC device under various scan rates. The CV curve of all the scan rates exhibited quasi-rectangular characteristics, indicating the formation of electric double layer and ideal capacitance behaviour of device. The volumetric capacitance of the bulk SC shows a maximum value of 0.33 mF cm^{-3} at 10 mV s^{-1} (Fig. S5b). When the scan rate increases, the volumetric capacitance value decreases. The minimum capacitance value of 0.10 mF cm^{-3} is found at 300 mV s^{-1}. The estimated volumetric capacitances of bulk SC are 0.24, 0.20, 0.18, 0.16, and 0.12 mF cm^{-3} with a scan rate of 50, 70, 100, 200 and mV s^{-1}, respectively.

Fig. S5c illustrates the GCD profiles of the bulk SC using various current densities (from 0.57 to 1.1 μA cm^{-2}). The GCD plots show a quasi-triangular shape in all the current values. The volumetric capacitance of bulk SC using GCD plots also estimated and the values are 0.19, 0.16, 0.13, 0.12 and 0.11 mF cm^{-3} at the current densities of 1.7, 2.1, 2.4, 2.8 and 3.2 μA cm^{-2}, respectively. The bulk SC also exhibited the volumetric capacitance value drops when the current density increases. In order to estimate the ion transport property in the bulk PVA-KOH, electrochemical impedance spectroscopy was studied on bulk SC device. In this study, a bulk PVA-KOH with a thickness of 0.18 mm was used. Fig. S5d shows the Nyquist plot of bulk SC that was measured before (pristine state) and after all electrochemical studies. The ionic conductivity of the bulk SC was found to be of the order of 10^{-8} S cm^{-1} at pristine state. After all electrochemical studies, the ionic conductivity of the device increased with the order of 10^{-7} S cm^{-1}. Indeed, the ionic conductivity of bulk SC exhibited lower value, which is nearly five orders of magnitude smaller than that of the thin planar MSC. The energy density (E_V) and power density (P_V) of the bulk SC was estimated from the GCD data and shown in Fig. S5e. The bulk SC exhibits a maximum volumetric energy density and power density of 0.027 mWh cm^{-3} and 0.031 W cm^{-3}, respectively, which is much smaller relative to that of the single-cell planar MSC device.

For better understanding, the positive cyclic sweep is labeled from A to C. Initially, the device was swept at constant sweep rate to certainly align the cation/anion in the respective electrode-electrolyte interfaces, in which the electrostatic interaction originates at the interfacial regime. After cycling test, the open circuit potential (OCP) study was immediately performed. The OCP with various sweep rates was also conducted in order to estimate the concentration of ionic charges on the origin of emf.

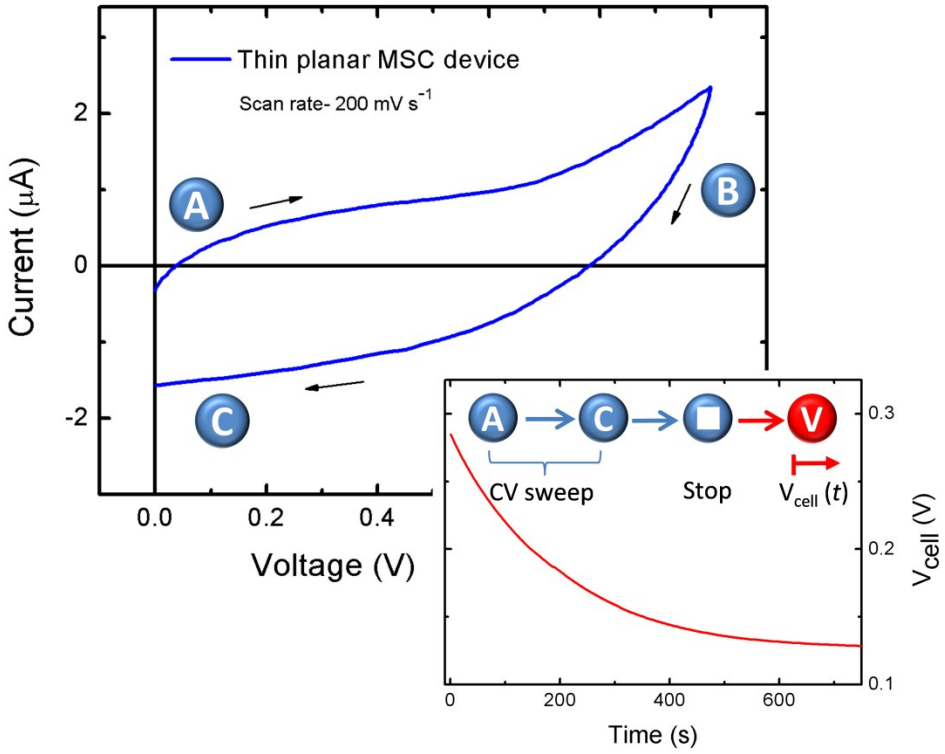

Fig. S6 Cyclic voltammetry and open circuit potential studies on a planar MSC device.

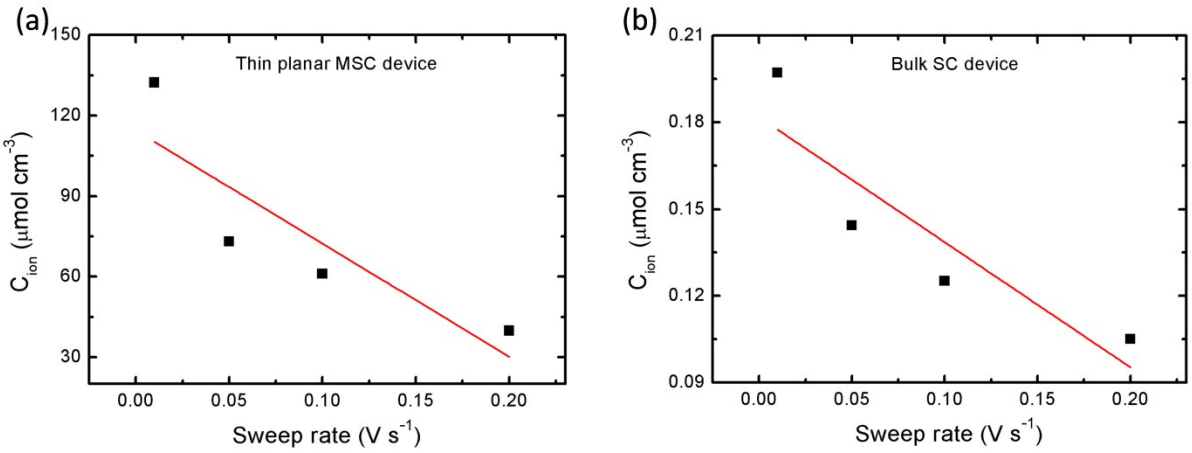

Fig.S7 Sweep rate dependent ionic concentration of (a) Thin planar MSC, and (b) Bulk SC device.

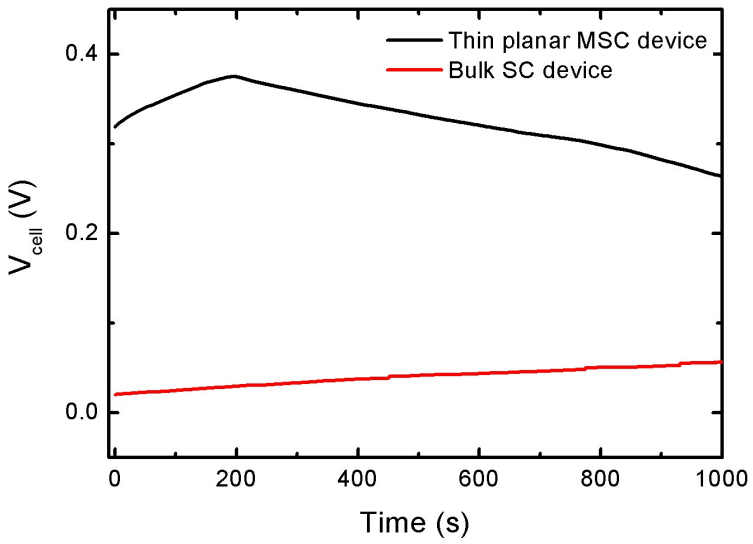

Fig. S8 The cell voltage (V_{cell}) as function on time was conducted on both thin planar MSC and bulk SC device under pristine state (without applying a positive cyclic sweep).

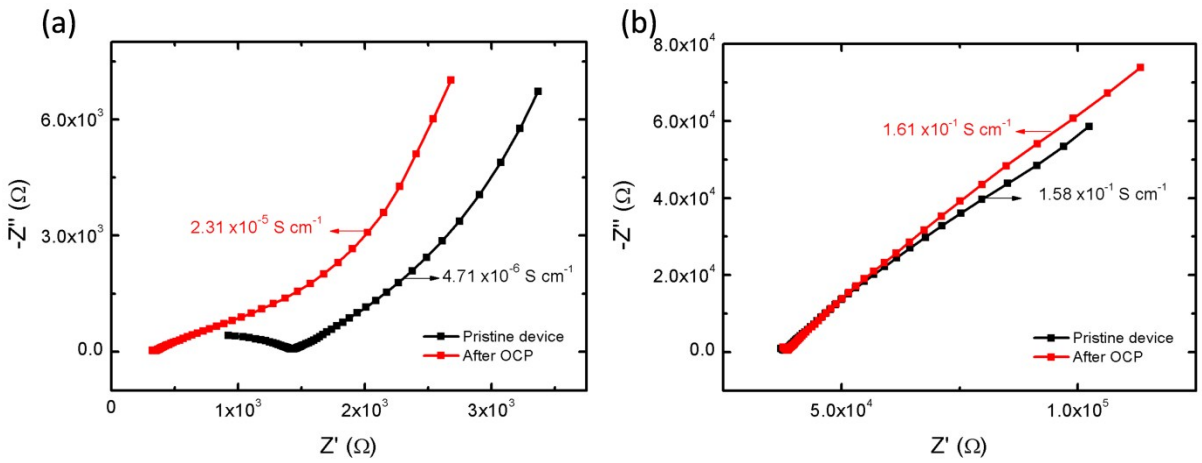

Fig. S9 Nyquist plots (a) Bulk SC and (b) Planar MSC devices measured before and after OCP studies. The thicknesses of bulk and thin PVA-KOH are 0.12 mm and 100 nm, respectively.

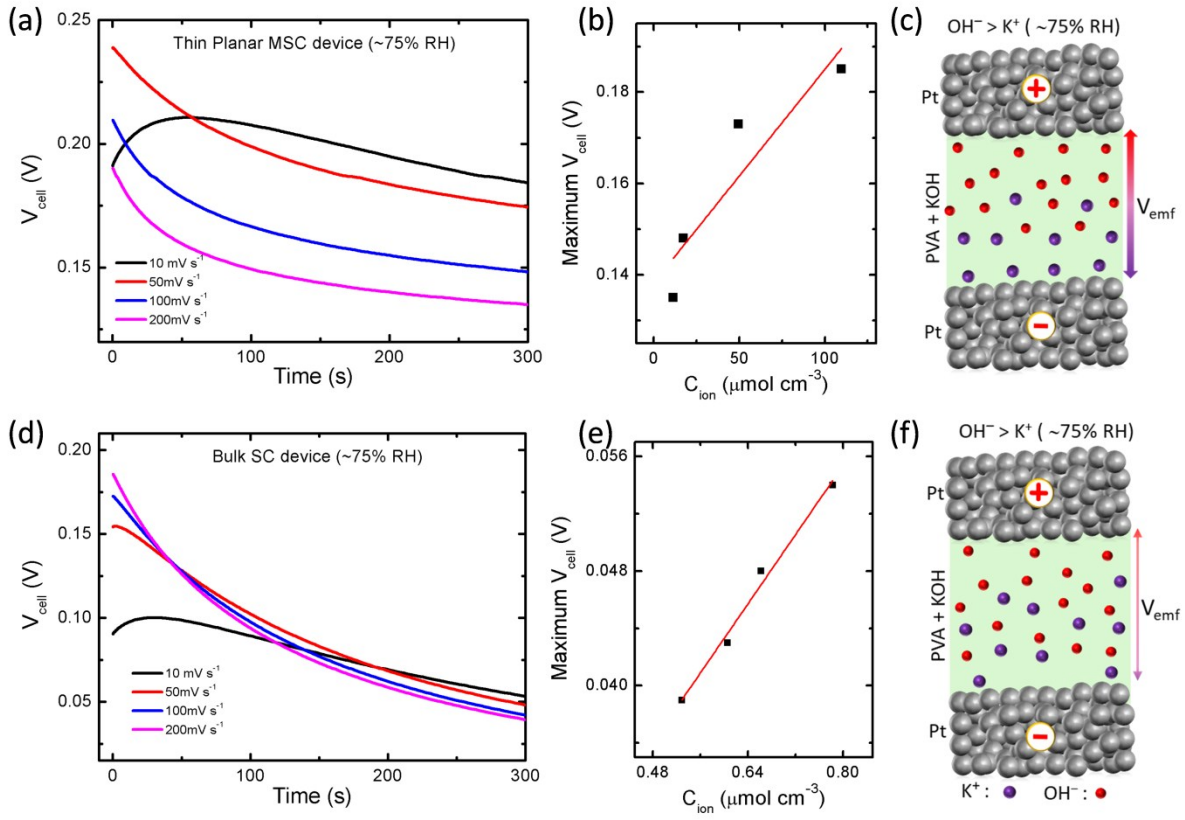

Fig. S10 Time dependent cell voltage (V_{cell}) measured under various relative humidity (RH%) and CV sweep rates in (a & d) Thin Pt/PVA-KOH/Pt planar MSC and bulk Pt/PVA-KOH/Pt SC, respectively. The OCP was performed after a single sweep in the positive voltage with different sweep rates. (b & e) Shows the maximum V_{cell} as function of ionic contribution (after equilibration) in the thin and bulk device, respectively (estimated using the relation 1). (c & f) Schematic representation of how V_{emf} is originated by the non-equilibrium ionic contribution (~75% RH) in the thin planar MSC and bulk SC devices, respectively.

Table S1. Supercapacitance characteristics are compared with the previously available reports.

Ref. No.	Electrode	Electrolyte	Specific Capacitance (Cs)
[1]	SWCNT	PVA-H_3PO_4	1 F cm^{-3} at 100 V s^{-1}
[2]	RGO	PVA-H_3PO_4	359 F cm^{-3} at 0.005 V s^{-1}
[3]	Direct laser write porous carbon	PVA-H_3PO_4	0.24 F cm^{-3} at 0.01 V s^{-1}
[4]	SWCNT	3.6 M H_2SO_4	1.04 F cm^{-3}
[5]	PEDOT	PVA–H_2SO_4	145 F cm^{-3}
[6]	Electrochemically reduced graphene oxide	25% KOH	0.24 F cm^{-3} at 40 µA cm^{-2}
[7]	Transparent carbon film	PVA-H_3PO_4	409 mF cm^2 (branched CNC)
[8]	RGO-CNT (9:1)	3 M KCl	3 F cm^{-3}at 50 V/ s
[9]	MWCNT	PVA-H_3PO_4-H_2O &0.5 M H_2SO_4	1.8 mF/cm^2
[10]	Onion-like carbon	Et_4NBF_4/anhydrous propylene carbonate electrolyte	0.9 mF/cm^2 at 100 V/s
-	This work	PVA-KOH	5.39 F cm^{-3} at 10 mV s^{-1}

The galvanostatic charging and discharging profiles of the planar MSC growth to effectively lights up a blue LED can be seen in the real-time movies **Pt_PVA-KOH_Pt planar MSC.mp4**.

References

1 J. Pu, X. Wang, R. Xu, K. Komvopoulos, *ACS Nano,* 2016, **10**, 9306–9315.

2 Z. Niu, L. Zhang, L. Liu, B. Zhu, H. Dong, X. Chen, *Adv. Mater*., 2013, **25**, 4035–4042.

3 J. B. In, B. Hsia, J. -H. Yoo, S. Hyun, C. Carraro, R. Maboudian, C. P. Grigoropoulos, *Carbon*, 2015, **83**, 144–151

4 K. U. Laszczyk, K. Kobashi, S. Sakurai, A. Sekiguchi, D. N. Futaba, T. Yamada, K. Hata, *Adv. Energy Mater*., 2015, **5**, 1500741

5 B. Anothumakkool, R. Soni, S. N. Bhange, S. Kurungot, *Energy Environ. Sci.,* 2015, **8**, 1339–1347.

6 K. Sheng, Y. Sun, C. Li, W. Yuan, G. Shi, *Sci. Rep*., 2012, **2**, 247.

7 H. Y. Jung, M. B. Karimi, M. G. Hahm, P. M. Ajayan, Y. J. Jung, *Sci. Rep*., 2012, **2**, 773.

8 M. Beidaghi, C. Wang, *Adv. Funct. Mater*., 2012, **22**, 4501–4510.

9 T. M. Dinh, D. Pech, M. Brunet, A. Achour, *J. Phys.: Conf. Ser*., 2013, **476***,* 012106.

10 D. Pech, M. Brunet, H. Durou, P. Huang, V. Mochalin, Y. Gogotsi, P. -L. Taberna, P. Simon, *Nat. Nanotechnol*., 2010, **5**, 651–654.